Journal of Anatomy

J. Anat. (2011) **218**, pp600–607 doi: 10.1111/j.1469-7580.2011.01374.x

The organisation of elastin and fibrillins 1 and 2 in the cruciate ligament complex

Kinley D. Smith,[1] Anne Vaughan-Thomas,[1]‡ David G. Spiller,[2] John F. Innes,[1] Peter D. Clegg[1] and Eithne J. Comerford[1]

[1]*Department of Musculoskeletal Biology, Institute of Aging and Chronic disease and School of Veterinary Science, Leahurst Campus, University of Liverpool, Liverpool, UK*
[2]*Centre for Cell Imaging, University of Liverpool, Liverpool, UK*

Abstract

Although elastin fibres and oxytalan fibres (bundles of microfibrils) have important mechanical, biochemical and cell regulatory functions, neither their distribution nor their function in cruciate ligaments has been investigated. Twelve pairs of cruciate ligaments (CLs) were obtained from 10 adult dogs with no evidence of knee osteoarthritis. Elastic fibres were identified using Verhoeff's and Miller's staining. Fibrillins 1 and 2 were immunolocalised and imaged using confocal laser scanning microscopy. Hydrated, unfixed tissue was analysed using Nomarski differential interference microscopy (NDIC), allowing structural and mechanical analysis. Microfibrils and elastin fibres were widespread in both CLs, predominantly within ligament fascicles, parallel to collagen bundles. Although elastin fibres were sparse, microfibrils were abundant. We described abundant fibres composed of both fibrillin 1 and fibrillin 2, which had a similar pattern of distribution to oxytalan fibres. NDIC demonstrated complex interfascicular and interbundle anatomy in the CL complex. The distribution of elastin fibres is suggestive of a mechanical role in bundle reorganisation following ligament deformation. The presence and location of fibrillin 2 in oxytalan fibres in ligament differs from the solely fibrillin 1-containing oxytalan fibres previously described in tendon and may demonstrate a fundamental difference between ligament and tendon.
Key words: cruciate ligament; elastin; fibrillin; microfibril.

Introduction

Cruciate ligaments (CLs) are dense bands of collagenous tissue that are the primary stabilisers of the knee (femorotibial) joint. The two components are anterior and posterior cruciate ligaments, with the anterior cruciate ligament (ACL) twisted around the posterior cruciate ligament (PCL) forming the CL complex (Arnoczky & Marshall, 1977). Each CL comprises multiple fascicles containing bundles of collagen fibres (Kennedy et al. 1974; Yahia & Drouin, 1989; Amis & Dawkins, 1991). Collagen fibres are not recruited isometrically during knee joint motion and each change in knee joint position recruits fibres differently (Amis & Dawkins, 1991; Butler et al. 1992). Although collagen provides tensile strength to the ligament complex, other structural components likely contribute to the overall mechanical function of the complex (Frank, 2004). Microfibrils (MFs), polymers of fibrillins 1 and 2, are considered to have a structural role in ligament and tendon. Bundles of MFs are known as oxytalan fibres. Elastin fibres comprise a central cross-linked core of highly extensible elastin surrounded by a supporting sheath of MFs, with many other associated molecules (Kielty, 2006). Collectively, oxytalan and elastin fibres are referred to as elastic fibres. Elastin has traditionally been considered a minor component of ligament tissue (Frank, 2004). A wide distribution of elastic fibres in the human ACL has been described (Strocchi et al. 1992). In canine CLs, only small numbers of elastin fibres have been reported (Paatsama, 1952; Vasseur et al. 1985).

Elastic fibres have important mechanical, biochemical and cell-regulatory functions in tissue. Reversible elasticity is a function of both elastin and oxytalan fibres and is dependent on water and calcium (Eriksen et al. 2001). MFs are stiffer than elastic fibres (Sherratt et al. 2003) and are highly resistant to axial tension (Glab & Wess, 2008). Distribution

Correspondence
Kinley D. Smith, Small Animal Hospital, Faculty of Veterinary Medicine, University of Glasgow, 464 Bearsden Road, Glasgow G61 1QH, UK. T: +44 (0) 141 330 5848; F: +44 (0) 141 330 3663; E: k.smith@vet.gla.ac.uk
‡Dr Vaughan-Thomas is deceased.

Accepted for publication *11 March 2011*
Article published online *6 April 2011*

of elastic fibres in tissue is considered to reflect function (Kielty et al. 2002). Regions of canine superficial digital flexor tendon (SDFT) that undergo the greatest strain deformation have the highest regional elastin content (Ritty et al. 2002). MFs also have key roles in extracellular regulation of transforming growth factor (TGF) β (Charbonneau et al. 2004) and cell adhesion (Ito et al. 1997; Wendel et al. 2000).

In the canine SDFT, fibrillin 1 is predominantly found in fibre form, and elastin and fibrillin 2 predominantly pericellularly. Fibrillin 2 is commonly found in MFs in foetal tissues but has been considered to have limited distribution in adult tissue (Cain et al. 2006). A recent study has suggested microfibrils in post-natal tissue may comprise a fibrillin 2 core and a fibrillin 1 outer sheath (Charbonneau et al. 2010b). Failure of elastic fibres has been implicated in a number of serious diseases (Kielty, 2006).

In this study, we use histology and immunofluorescence to detail methodically the distribution of elastic fibres and fibrillins 1 and 2 in the canine CL complex. We also use micromechanical manipulation and enzymatic digestion to explore CL microanatomy. By understanding the distribution and function of these molecules in the CL complex, we intend to gain a greater understanding of CL physiology, providing valuable insight into the aetiopathogenesis of non-contact ACL injury and information for future ligament engineering projects in mammalian species.

Materials and methods

Sample collection and preparation

Twelve pairs of ACLs and PCLs were harvested from 10 skeletally mature Greyhounds with no macroscopic evidence of any knee joint pathology or of systemic disease. The animals were euthanised for reasons not related to this study with informed consent obtained according to standard University ethical review. Six pairs of CLs from five dogs were sectioned into proximal, middle and distal sections, embedded on cork discs in Tissue-Tek OCT (Sakura Finetek, Torrance, CA, USA) and immediately snap-frozen in isopentane using liquid nitrogen, then stored at −80 °C until immunofluorescence staining and NDIC analysis. Six pairs of CLs from five dogs were fixed in 4% paraformaldehyde (P6148; Sigma-Aldrich, UK) for 24 h, then embedded in paraffin before sectioning for histological examination.

Histology

Sequential 4-μm sections from paraffin-embedded samples were stained with

- haematoxylin and eosin (H&E) to allow assessment of tissue morphology
- Verhoeff's iodine-iron haematoxylin (EVH) to assess distribution of elastin fibres
- Miller's stain (M) to allow assessment of both elastin and oxytalan fibres

This staining methodology was used to allow assessment of tissue architecture and, through comparison of EVH- and M-stained sections, differentiation of elastin and oxytalan fibres (Barros et al. 2002). Images were recorded on a dedicated microscope (Nikon Eclipse 80i). H&E sections were assessed by two observers blinded to sample information (K.D.S. and E.J.C.) for signs of CL degeneration according to criteria detailed previously (Vasseur et al. 1985). Briefly, this involved awarding a score from 0 to 3 according to the following criteria:

- Grade 0: healthy ligament
- Grade 1: mild degenerate changes with focal loss of collagen architecture
- Grade 2: moderate degeneration with regional disruption to collagen architecture and Grade 3: severe degeneration affecting large sections of ligament.

Antibodies

Two antibodies were used to immunostain fibrillins 1 and 2 and elastin. Antibodies against fibrillin 1 were rabbit polyclonal antibodies raised against the proline-rich domain (Trask et al. 1999) and toward the carboxyterminal domain of human fibrillin 1 (Ritty et al. 1999), respectively. Antibodies against fibrillin 2 were both rabbit polyclonal antibodies raised against the glycine-rich region of human fibrillin 2 and against amino acids Met-1 to Thr-1114 of human fibrillin 2, respectively (Trask et al. 1999). All four fibrillin antibodies have been affinity-purified and do not cross-react (Ritty et al. 2002). Immunolabelling of elastin was achieved using two commercial antibodies (ab9519, monoclonal mouse IgG; Abcam, UK, 1 : 100, and E4013, monoclonal mouse IgG, Sigma-Aldrich).

Immunofluorescence

Longitudinal and transverse 30-μm sections were cut from six pairs of CLs from five dogs on a cryostat (Bright OTF 5000) and transferred to poly-L-lysine slides (Polysine, VWR, UK). Tissue was fixed overnight in 100% methanol at −20 °C, then slides were rinsed in distilled water and allowed to dry prior to staining. Cold methanol fixation was used for immunohistochemistry, as paraformaldehyde markedly reduced antibody binding. Sections were rehydrated in phosphate-buffered saline (PBS), pH 7.4 for 5 min, then incubated with hyaluronidase (4800 IU mL^{-1} in PBS, H3884; Sigma-Aldrich) with a protease inhibitor cocktail (P2714; Sigma-Aldrich) for 24 h at room temperature, then rinsed for 5 min, three times in PBS. A second incubation with collagenase (30 IU mL^{-1} in PBS, C2674; Sigma-Aldrich) for 30 min was followed by a further PBS rinsing. Enzymatic digestion improved visualization of elastin and, to a lesser extent, fibrillin 1. Sections were blocked with 5% normal goat serum (PCN5000; Invitrogen, CA, USA) for 1 h at room temperature, then incubated with a solution of two antibodies raised against elastin (ab9519 at 1 : 100 and E4013 at 1 : 5000) overnight at 4 °C in a humidity chamber. A second incubation with antibodies against fibrillin 1 or 2 (1 : 50) overnight at 4 °C was followed by rinsing in PBS and incubation for 1 h at room temperature with anti-mouse IgG-conjugated Alexafluor 488 (1 : 500, A11001; Invitrogen) and anti-rabbit IgG-conjugated Alexafluor 568 (A11011; Invitrogen). Sections were rinsed in PBS before mounting in DAPI-containing medium (H-1500, Vectashield, Vector Laboratories, UK). Negative controls were

Fig. 1 (A) Distribution of elastin fibres in the CL complex, longitudinal section, ACL ×100 Verhoeff's stain. Sparse elastin fibres (arrowheads) orientated parallel to collagen bundles. Scale bar: 40 μm. (B) Distribution of elastin fibres in the CL complex, longitudinal section, PCL ×100 Verhoeff's stain. Short elastin fibres (arrowheads) are seen running obliquely between two collagen bundles. Scale bar: 40 μm. (C) Distribution of elastin fibres in the CL complex, longitudinal section, ACL ×100 stained with antibodies to elastin. Perpendicular fibres of elastin (stained green; yellow arrowheads) spanning an interbundle region (edge of collagen bundles marked by black lines). Notice the similarity to the interbundle fibres stained histochemically in (B). Scale bar: 40 μm. (D) Distribution of microfibrils in the canine CL complex, longitudinal section, PCL, Miller's stain: Larger elastin fibres (blue arrows) are seen parallel to collagen bundles. Finer microfibrils (black arrowheads) run obliquely and vary in size. The field contains many fine microfibrils, many of which are only just visible at this Scale. Scale bar: 40 μm. (E) Distribution of microfibrils in the canine CL complex, transverse section, ACL, Miller's stain. Microfibrils (black dots; blue arrow) abundant within the collagen bundles. Scale bar: 40 μm. (F) Distribution of fibrillin-1 in the canine CL complex, longitudinal section, ACL, × 100, no enzymatic pre-treatment. Fibrillin-1 (red) forms fibres. Scale bar: 40 μm. (G) Distribution of fibrillin-1 in the canine CL complex, longitudinal section, ACL × 63 CLSM image, enzymatic pre-treatment: Fibrillin 1 (orange) is found pericellularly where nuclei are rounded (nuclei in blue). Staining of fibrillin 1 is also seen extending parallel to collagen in a fibre-like structure (arrows) from an elongated nucleus. Although some co-localisation (yellow) is seen with elastin (green), elastin fibres were generally found to contain little fibrillin 1. Scale bar: 50 μm. Images H–K taken from a single longitudinal section, Greyhound ACL, × 100. (H) Elastin and fibrillin 1 rarely co-stain when in fibre form. Fibrillin 1 (red) forming fibres (yellow arrowheads). (I) Elastin (green) forming fibres (yellow arrowheads). (J) Combined image of A and B showing lack of co-localisation of fibrillin 1 and elastin in fibre form. (K) Light image showing detail of collagen bundles. Both fibrillin 1 and elastin fires run parallel with collagen bundles. Scale bars H–K: 40 μm. (L) Distribution of fibrillin-2 in the canine CL complex, longitudinal section, ACL × 63 CLSM image from fascicular region showing fibrillin-2 (red) in long and dense fibres broadly aligned with collagen bundles, with some branching. Nuclei are stained with DAPI (blue). Scale bar: 50 μm (M) Distribution of fibrillin-2 in the canine CL complex, longitudinal section, PCL, × 40. Fibrillin-2 (red) shows a highly branched pattern. Scale bar: 100 μm. Images N and O taken from a single longitudinal section, ACL, × 100. (N) Co-staining of elastin and fibrillin 2. Two brightly staining parallel elastin fibres are noted (green; yellow arrowheads) with one solitary faint staining elastin fibre (green; red arrowhead). Scale bar: 40 μm. (O) Co-staining of elastin and fibrillin 2. Two fibrillin 2 fibres corresponding to the elastin fibres are noted (white arrows). There is a fibrillin 2 fibre corresponding to the faint elastin fibre (yellow arrow). The majority of fibrillin 2 fibres do not co-stain for elastin. Scale bar: 40 μm.

achieved by omitting the primary or secondary antibody and one or both enzymatic digestions (data not presented). Positive controls for elastin were performed on elastin-rich vascular tissue where the distribution of elastin could be compared to histochemically stained sections (data not presented). All four fibrillin antibodies have been validated previously in canine connective tissue (Ritty et al. 2002).

Nomarski differential interference contrast optical microscopy (NDIC)

Unfixed 30-μm cryosections from six pairs of CLs from five dogs were transferred to slides and kept moist using lactated Ringer's solution (Aquapharm No.11; Animalcare, UK). Fabric tabs were attached to the sections using superglue to allow application of transverse and longitudinal strain. Strain was measured relative to the width of the tissue sample in the direction of strain application and strain was progressively applied to 300%. Lactated Ringer's was applied to the section before applying a coverslip. Images were recorded on a dedicated microscope (Nikon Eclipse 80i). This facilitated manipulation of unfixed tissue within a physiological solution where the elasticity of elastic fibres was preserved as described previously (Pezowicz et al. 2005; Pezowicz et al. 2006).

Imaging

Two-dimensional images were collected on a dedicated microscope (Nikon Eclipse 80i) using ×10, ×40 or ×100 objective lenses. A confocal laser scanning microscope (CLSM) (Zeiss LSM 510 META NLO) was used to obtain three-dimensional images. A ×63 oil immersion lens was used, and two-dimensional images are presented as projections of three dimensional stacks.

Results

Animals

Of the 10 dogs, six were male and four female. Seven pairs of CLs were from the male dogs and five pairs of CLs from the female dogs. Ages ranged from 32 to 68 (median 35) months, and all had been in training for racing prior to being subjected to euthanasia.

H&E sections

All ACLs and PCLs from six knees were assessed as having a low level of degenerative change (Grade I by both assessors according to Vasseur scale). Staining of collagen throughout the ligaments demonstrated no loss of density or disruption to the collagen architecture.

Elastin fibres (EVH)

Elastin fibres were distributed consistently throughout both ACLs and PCLs with little variation within CLs, between ACLs and PCLs or between CLs of differing joints or dogs. Increased numbers of elastin fibres were observed in the epiligament. This increased staining was uniform in degree and pattern in the surface layers of both CLs. Within the substance of both CLs, elastin fibres varied in width and orientation and most were orientated parallel to collagen bundles (Fig. 1A). Elastin fibres were more commonly found on the surface of rather than within collagen bundles. Increased elastin fibre staining was observed in interbundle

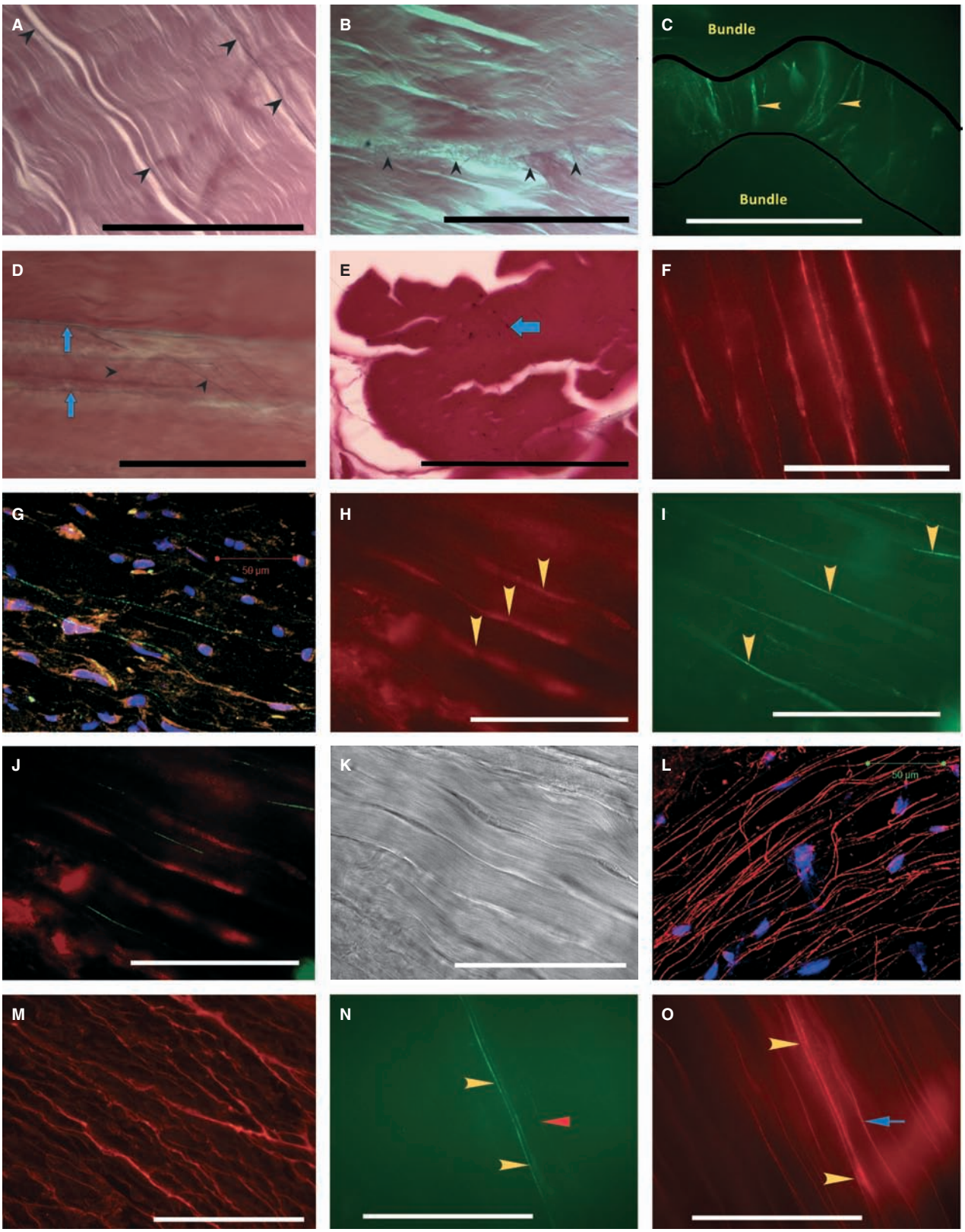

regions (Fig. 1B). Interbundle elastin fibres were orientated either perpendicular or oblique to collagen bundles and were either straight or tortuous (Fig. 1C). Elastin fibres were abundant in interfascicular regions and were loosely organised. Elastin fibres could not be imaged without dual enzymatic digestion.

Oxytalan fibres (Miller's stain)

Oxytalan fibres were more numerous and finer than elastin fibres throughout both CLs. No differences were noted in oxytalan staining between proximal, middle and distal CLs, between ACLs and PCLs or between knees or dogs. Oxytalan fibres were found in the epiligament, subjectively at greater frequency than that observed in the substance. Fibres were broadly orientated along the axis of the underlying collagen bundles, but significant numbers of fibres were oblique and perpendicular. Within the substance of the CL, large numbers of fibres were observed running parallel to collagen bundles, and were often only just visible at the very limit of resolution of the microscope at ×100 oil-immersion magnification (Fig. 1D). The majority of fibres in the interfascicular region were arranged in a fine, tortuous meshwork with no overall orientation, although some ran perpendicularly between bundles. Oxytalan fibres were commonly found both on the outside and within collagen bundles, where again there was marked variation in diameter (Fig. 1E).

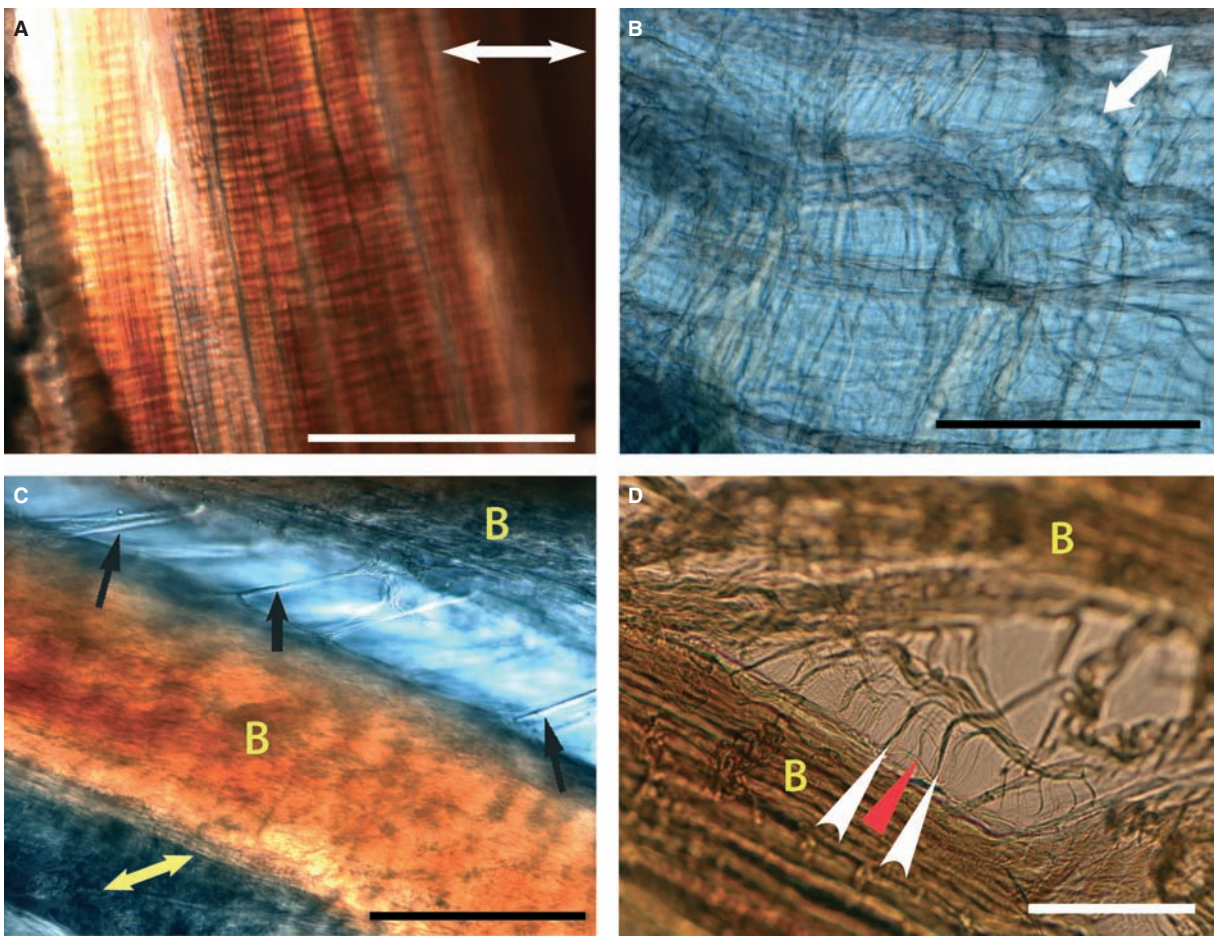

Fig. 2 Images (A) and (B) taken simultaneously from adjacent regions under identical stress, demonstrating variation in ligament strain during constant stress in the ACL in fully hydrated, unfixed tissue, longitudinal sections. Double-headed white arrows indicate direction of applied stress. (A) Tightly adherent collagen bundles with no lateral separation with stress applied perpendicularly to collagen bundles. Scale bar: 100 μm (B) Interfascicular region demonstrating loose but organised tissue following application of stress perpendicular to ligament fascicles. Interfascicular fibres run obliquely to fascicles in both directions. Scale bar: 100 μm. (C) Variation in interbundle strain during application of perpendicular stress in the CLs in fully hydrated, unfixed tissue, longitudinal section, PCL × 40. Direction of applied strain is shown by yellow double-headed arrow. Collagen bundles are marked as yellow 'B'. Straight, thick transverse interbundle fibres (black arrows) are seen. Scale bar: 100 μm (D) Variation in interbundle strain during application of perpendicular stress in the CLs in fully hydrated, unfixed tissue, longitudinal section, ACL × 40. Collagen bundles are marked as yellow 'B'. Unilateral oblique interbundle fibres (white arrowheads). Subdivision of these oblique fibres is noted (red arrowhead). Scale bar: 40 μm.

Fibrillins

Fibrillin 1 was consistently found throughout both ACL and PCLs. In sections that had not undergone enzymatic digestion, fibrillin 1 was seen to form fibres throughout both CLs (Fig. 1F). These fibres were often markedly branched. Dense fibre staining was seen throughout interfascicular regions where fine fibres formed a dense, irregular meshwork, similar to that previously described for histochemical microfibril staining. Where nuclei were round, fibrillin 1 was found only pericellularly (Fig. 1G). Co-localisation with elastin was commonly seen pericellularly, but fibrillin 1 was rarely seen when the elastin was part of a fibre (Fig. 1H-K). In the epiligament fibrillin 1 was more abundant than was seen in the ligament substance. No interligament or regional variation was apparent. The staining intensity of fibrillin 1 was reduced slightly by collagenase but not by hyaluronidase enzymatic digestion.

Fibrillin 2 was organised in numerous fibres, broadly orientated parallel with collagen bundles, with occasional oblique fibres (Fig. 1L). These fibres were observed throughout ACL and PCLs and could also be highly branched (Fig. 1M). The pattern of distribution was similar to that of fibrillin 1. Where elastin fibres were seen, fibrillin 2 was commonly co-localised (Fig. 1N,O). However, the majority of fibrillin 2 fibres did not stain for elastin. Weak pericellular staining was occasionally noted throughout both CLs. No interligament or regional variation was apparent. Fibrillin 2 fibres were present on sections without collagenase and hyaluronidase treatment and staining was unaffected by enzymatic digestion.

NDIC

Perpendicular stretching of hydrated unfixed ligament under NDIC revealed complex interconnections between collagen bundles and fascicles when compared to unstrained tissue. These changes were consistent between CLs and between dogs. When the whole diameter of the ligament was subjected to lateral stress, all of the strain was observed in the interfascicular regions (Fig. 2A,B). The collagen bundles remained tightly opposed, whereas the interfascicular region showed loose but organised fibres.

When individual fascicles were fixed, perpendicular strain allowed observation of interbundle anatomy. With minimal strain, residual fibres were seen running transversely (Fig. 2C), obliquely in one direction (Fig. 2D) or obliquely in both directions. Following the removal of the lateral stress, the bundles recoiled spontaneously. Further separation of collagen bundles separated the oblique fibres into S-shaped subdivisions which were again reversible following the removal of lateral stress. Fibres that spanned interbundle regions transversely could be found with or without oblique fibres and could be anchored by a single point on a collagen fibre or a more diffuse and complex attachment deeper into the bundle.

Discussion

In this study we have demonstrated the widespread presence of elastic fibres, elastin, and fibrillins 1 and 2 in the canine CL complex. Analysis of subdivisions of the CL complex has demonstrated abundant oxytalan fibres and that these have a similar pattern of distribution to the fibres comprising fibrillins 1 and 2.

Elastin fibres were found throughout both ACL and PCLs and were abundant in the interbundle and interfascicular regions. Sparse fibres within bundles are unlikely to contribute to the mechanical strength of the ligament but may provide additional stiffness at low strain and stress (Smith & Fazzalari, 2006). In the periodontal ligament, elastin fibres have been suggested to provide mechanical support to the vascular network, restoring vessel shape following deformation (Sawada et al. 2006). During ligament micro-movement, blood vessels are thought to be occluded (O'Donoghue et al. 1971; Kobayashi et al. 2006) and such elastic mechanical support may also be important in the CL. Whereas elastin fibres were only rarely found within bundles, oxytalan fibres were abundant. Certainly the high density of oxytalan fibres within collagen bundles would suggest some role in mechanical ligament function such as absorption of low strain stiffness, complementing the tensile strength of collagen fibres, or restoration of longitudinal conformation following longitudinal strain (Karlinsky et al. 1976; Oakes & Bialkower, 1977; Oxlund & Andreassen, 1980; Oxlund et al. 1988; Lee et al. 2001).

Where elastin formed part of an elastin fibre, fibrillin 2 but not fibrillin 1 commonly co-localised. The authors believe the pattern of fibrillin 2 staining was similar to both fibrillin 1 and oxytalan fibre distribution throughout the CLs. The density and distribution of oxytalan fibres was similar in histochemically stained and immunofluorescence sections (compare Figs 2B,D). Thus fibrillin 2 appears to be a significant component of microfibrils in canine CL. As the MF is a key component of the elastin fibre, this explains the co-localisation of elastin and fibrillin 2. However, immunostaining of fibrillin 1 revealed fibres likely to be microfibrils (Kielty, 2006; Yu et al. 2007) but there was very little fibrillin 1 staining associated with elastin fibres. Collagenase digestion has been shown to remove fibrillin 1 from the MF, potentially exposing the fibrillin 2 core (Charbonneau et al. 2010b), but in this study it resulted in a reduction in the intensity of fibrillin 1 staining. As collagenase digestion was required to immunostain elastin, this may have disrupted the fibrillin 1 staining pattern.

In the canine CL complex, the distribution of fibrillin 1 and 2 differs from that described in other tissues. Fibrillin 2 has been considered to have limited distribution in adult tis-

sue (Cain et al. 2006) but MFs may comprise an inner core of fibrillin 2 surrounded by fibrillin 1 (Charbonneau et al. 2010b). In canine SDFT, only fibrillin 1 was observed to form fibres (Ritty et al. 2002). However, the unmasking of the fibrillin 2 epitope may be a marker for MF degeneration (Charbonneau et al. 2010a). Canine CLs commonly have histologic changes considered to be degenerative (Vasseur et al. 1985; Comerford et al. 2006) and the widespread fibre pattern may reflect degeneration of the CL ECM unmasking fibrillin 2.

When imaging the variation in interfascicular and interbundle anatomy in unfixed, hydrated tissue the fibres of the interfascicular region appear loosely organised and may allow fascicles to move freely in relation to each other. Furthermore, the highly deformable nature of the interfascicular fibres could offer some stress protection for other structures such as blood vessels and nerves that run within these regions. Our observations show a hierarchical subdivision of interbundle fibres similar to that described in the human annulus fibrosus (Pezowicz et al. 2005). We have shown interbundle and interfascicular fibres to contain elastin and oxytalan fibres histochemically and through immunofluorescence. These elements show strikingly similar anatomical distribution to the interbundle and interfascicular fibres we demonstrated on unfixed, hydrated CL using NDIC (compare Figs 1C and 2C). We have also shown the interbundle and interfascicular fibres to have elastic properties. Therefore it is not unreasonable to assume that these fibres contain elastin and oxytalan fibres. A passive recoil system formed from elastin and oxytalan fibres offers a mechanism whereby ligament anatomy can be restored following deformation. Such a mechanism has been proposed in the heart valves (Vesely, 1998) and annulus fibrosus (Cloyd & Elliott, 2007; Yu et al. 2007).

In summary, we have shown that elastic fibres may have potentially important mechanical roles in this ligament complex. We described abundant oxytalan fibres composed of both fibrillin 1 and 2 and have suggested this differs from the solely fibrillin 1-containing oxytalan fibres previously described in tendon. The presence and location of fibrillin 2 in MFs in ligament may demonstrate a fundamental difference between ligament and tendon.

Acknowledgements

Antibodies to fibrillins 1 and 2 were a kind gift from Dr Timothy Ritty (Penn State University). K.D.S. is funded by the BBSRC by a Doctoral Training Award, Grant BB/F017502/1.

References

Amis AA, Dawkins GP (1991) Functional anatomy of the anterior cruciate ligament. Fibre bundle actions related to ligament replacements and injuries. *J Bone Joint Surg Br* **73**, 260–267.

Arnoczky SP, Marshall JL (1977) The cruciate ligaments of the canine stifle: an anatomical and functional analysis. *Am J Vet Res* **38**, 1807–1814.

Barros EM, Rodrigues CJ, Rodrigues NR, et al. (2002) Aging of the elastic and collagen fibers in the human cervical interspinous ligaments. *Spine J* **2**, 57–62.

Butler DL, Guan Y, Kay MD, et al. (1992) Location-dependent variations in the material properties of the anterior cruciate ligament. *J Biomech* **25**, 511–518.

Cain SA, Morgan A, Sherratt MJ, et al. (2006) Proteomic analysis of fibrillin-rich microfibrils. *Proteomics* **6**, 111–122.

Charbonneau NL, Ono RN, Corson GM, et al. (2004) Fine tuning of growth factor signals depends on fibrillin microfibril networks. *Birth Defects Res C Embryo Today* **72**, 37–50.

Charbonneau NL, Carlson EJ, Tufa S, et al. (2010a) In vivo studies of mutant fibrillin-1 microfibrils. *J Biol Chem* **285**, 24943–24955.

Charbonneau NL, Jordan CD, Keene DR, et al. (2010b) Microfibril structure masks fibrillin-2 in postnatal tissues. *J Biol Chem* **285**, 20242–20251.

Cloyd JM, Elliott DM (2007) Elastin content correlates with human disc degeneration in the anulus fibrosus and nucleus pulposus. *Spine* **32**, 1826–1831.

Comerford EJ, Tarlton JF, Wales A, et al. (2006) Ultrastructural differences in cranial cruciate ligaments from dogs of two breeds with a differing predisposition to ligament degeneration and rupture. *J Comp Pathol* **134**, 8–16.

Eriksen TA, Wright DM, Purslow PP, et al. (2001) Role of Ca^{2+} for the mechanical properties of fibrillin. *Proteins* **45**, 90–95.

Frank CB (2004) Ligament structure, physiology and function. *J Musculoskelet Neuronal Interact* **4**, 199–201.

Glab J, Wess T (2008) Changes in the molecular packing of fibrillin microfibrils during extension indicate intrafibrillar and interfibrillar reorganization in elastic response. *J Mol Biol* **383**, 1171–1180.

Ito S, Ishimaru S, Wilson SE (1997) Inhibitory effect of type 1 collagen gel containing alpha-elastin on proliferation and migration of vascular smooth muscle and endothelial cells. *Cardiovasc Surg* **5**, 176–183.

Karlinsky JB, Catanese A, Honeychurch C, et al. (1976) In vitro effects of elastase and collagenase on mechanical properties of hamster lungs. *Chest* **69**, 275–276.

Kennedy JC, Weinberg HW, Wilson AS (1974) The anatomy and function of the anterior cruciate ligament. As determined by clinical and morphological studies. *J Bone Joint Surg Am* **56**, 223–235.

Kielty CM (2006) Elastic fibres in health and disease. *Expert Rev Mol Med* **8**, 1–23.

Kielty CM, Baldock C, Lee D, et al. (2002) Fibrillin: from microfibril assembly to biomechanical function. *Philos Trans R Soc Lond B Biol Sci* **357**, 207–217.

Kobayashi S, Baba H, Uchida K, et al. (2006) Microvascular system of anterior cruciate ligament in dogs. *J Orthop Res* **24**, 1509–1520.

Lee TC, Midura RJ, Hascall VC, et al. (2001) The effect of elastin damage on the mechanics of the aortic valve. *J Biomech* **34**, 203–210.

Oakes VW, Bialkower B (1977) Biomechanical and ultrastructural studies on the elastic wing tendon from the domestic fowl. *J Anat* **123**, 369–387.

O'Donoghue DH, Frank GR, Jeter GL, et al. (1971) Repair and reconstruction of the anterior cruciate ligament in dogs. Factors influencing long-term results. *J Bone Joint Surg Am* **53**, 710–718.

Oxlund H, Andreassen TT (1980) The roles of hyaluronic acid, collagen and elastin in the mechanical properties of connective tissues. *J Anat* **131**, 611–620.

Oxlund H, Manschot J, Viidik A (1988) The role of elastin in the mechanical properties of skin. *J Biomech* **21**, 213–218.

Paatsama S (1952) *Ligamentous Injuries of the Canine Stifle Joint, a clinical and experimental study, Thesis*. Helsinki: Royal Veterinary College.

Pezowicz CA, Robertson PA, Broom ND (2005) Intralamellar relationships within the collagenous architecture of the annulus fibrosus imaged in its fully hydrated state. *J Anat* **207**, 299–312.

Pezowicz CA, Robertson PA, Broom ND (2006) The structural basis of interlamellar cohesion in the intervertebral disc wall. *J Anat* **208**, 317–330.

Ritty TM, Broekelmann T, Tisdale C, et al. (1999) Processing of the fibrillin-1 carboxyl-terminal domain. *J Biol Chem* **274**, 8933–8940.

Ritty TM, Ditsios K, Starcher BC (2002) Distribution of the elastic fiber and associated proteins in flexor tendon reflects function. *Anat Rec* **268**, 430–440.

Sawada T, Sugawara Y, Asai T, et al. (2006) Immunohistochemical characterization of elastic system fibers in rat molar periodontal ligament. *J Histochem Cytochem* **54**, 1095–1103.

Sherratt MJ, Baldock C, Haston JL, et al. (2003) Fibrillin microfibrils are stiff reinforcing fibres in compliant tissues. *J Mol Biol* **332**, 183–193.

Smith LJ, Fazzalari NL (2006) Regional variations in the density and arrangement of elastic fibres in the anulus fibrosus of the human lumbar disc. *J Anat* **209**, 359–367.

Strocchi R, de Pasquale V, Gubellini P, et al. (1992) The human anterior cruciate ligament: histological and ultrastructural observations. *J Anat* **180** (Pt 3), 515–519.

Trask TM, Ritty TM, Broekelmann T, et al. (1999) N-terminal domains of fibrillin 1 and fibrillin 2 direct the formation of homodimers: a possible first step in microfibril assembly. *Biochem J* **340** (Pt 3), 693–701.

Vasseur PB, Pool RR, Arnoczky SP, et al. (1985) Correlative biomechanical and histologic study of the cranial cruciate ligament in dogs. *Am J Vet Res* **46**, 1842–1854.

Vesely I (1998) The role of elastin in aortic valve mechanics. *J Biomech* **31**, 115–123.

Wendel DP, Taylor DG, Albertine KH, et al. (2000) Impaired distal airway development in mice lacking elastin. *Am J Respir Cell Mol Biol* **23**, 320–326.

Yahia LH, Drouin G (1989) Microscopical investigation of canine anterior cruciate ligament and patellar tendon: collagen fascicle morphology and architecture. *J Orthop Res* **7**, 243–251.

Yu J, Tirlapur U, Fairbank J, et al. (2007) Microfibrils, elastin fibres and collagen fibres in the human intervertebral disc and bovine tail disc. *J Anat* **210**, 460–471.